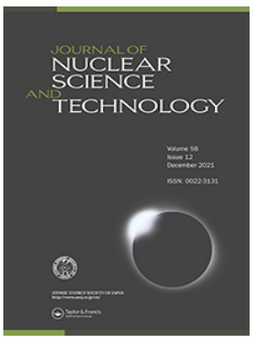

Journal of Nuclear Science and Technology

ISSN: (Print) (Online) Journal homepage: https://www.tandfonline.com/loi/tnst20

Integral experiments of technetium-99 using fast-neutron source reactor 'YAYOI'

Shoji Nakamura, Yuichi Hatsukawa, Atsushi Kimura, Yosuke Toh & Hideo Harada

To cite this article: Shoji Nakamura, Yuichi Hatsukawa, Atsushi Kimura, Yosuke Toh & Hideo Harada (2021) Integral experiments of technetium-99 using fast-neutron source reactor 'YAYOI', Journal of Nuclear Science and Technology, 58:12, 1318-1329, DOI: 10.1080/00223131.2021.1942278

To link to this article: https://doi.org/10.1080/00223131.2021.1942278

JOURNAL OF NUCLEAR SCIENCE AND TECHNOLOGY
2021, VOL. 58, NO. 12, 1318–1329
https://doi.org/10.1080/00223131.2021.1942278

ARTICLE

Integral experiments of technetium-99 using fast-neutron source reactor 'YAYOI'

Shoji Nakamura[a], Yuichi Hatsukawa[b], Atsushi Kimura[a], Yosuke Toh[a] and Hideo Harada[a]

[a]Nuclear Science and Engineering Center, Japan Atomic Energy Agency, Naka-gun, Ibaraki-ken, Japan; [b]Tokai Quantum Beam Science Center, National Institutes for Quantum and Radiological Science and Technology, Naka-gun, Ibaraki-ken, Japan

ABSTRACT

The present study performed integral experiments of ^{99}Tc by an activation method using a fast-neutron source reactor 'YAYOI' of the University of Tokyo to validate evaluated nuclear data libraries: JENDL-4.0, ENDF/B-VII and VIII. Technetium-99 samples were irradiated with reactor neutrons using a pneumatic system, and repeated 74 times to accumulate statistics. Reaction rates of ^{99}Tc were obtained by measuring decay gamma rays emitted from ^{100}Tc. The fast-neutron flux spectrum at the YAYOI was checked with flux monitors and MCNP calculations. The experimental reaction rate of ^{99}Tc was compared with the reaction rates given using both the fast-neutron flux spectrum and evaluated nuclear data libraries. The present integral experiments supported the evaluated nuclear data library JENDL-4.0.

ARTICLE HISTORY
Received 23 March 2021
Accepted 7 June 2021

KEYWORDS
Technetium-99; technetium-100; integral experiment; activation method; fast-neutron flux spectrum; fast-neutron source reactor; yayoi

1. Introduction

Radioactive wastes generated from spent nuclear fuels have been still an unsolved issue to people in the world. If the issue of the radioactive wastes was alleviated, it would approach social acceptance for nuclear reactors. In such a situation, nuclear transmutation can be considered one of candidates to solve the issue; transmutation can reduce an environmental load due to high-level wastes. If a fast-neutron reactor would be used, transmutation of fission products could be achieved with surplus neutrons while breeding. Various methods of transmutation using the fast-neutron reactor have been reported [1,2], and recently, the method to achieve high nuclear transmutation rate [3] has been reported for four nuclides of long-lived fission products: ^{79}Se, ^{99}Tc, ^{107}Pd, and ^{129}I. Reference [3] showed that efficient transmutation can be achieved for ^{99}Tc ($(2.111 \pm 0.012) \times 10^5$ yr [4].) by combining moderators and with use made of Tc itself as a thermal-neutron filter. In transmutation study using the fast-neutron reactor, neutron cross-section data with high accuracy and reliability are required in a fast-neutron energy region to evaluate transmutation rates. Hence, we examined the situation of the capture cross-section data of ^{99}Tc. Figure 1 plots neutron capture cross-sections adopted in evaluated nuclear data libraries [5–7] and past reported experimental data [8–13] in a fast-neutron energy region. There are discrepancies between the evaluated libraries in the neutron energy range of several keV to 250 keV, and especially JENDL-4.0 [5] and ENDF/B-VII.0 [6], -VIII.0 [7] libraries apparently differ from each other; cross-section data at a neutron energy of 100 keV are 0.3871 (b) in JENDL-4.0 and 0.6058 (b) in ENDF/B-VIII.0. Here, it shall be obvious that it is necessary to confirm which is correct, JENDL-4.0 or ENDF/B-VIII.0 evaluations. In conducting this verification, the authors had irradiation data of ^{99}Tc samples obtained in the past with a fast-neutron source reactor 'YAYOI' of the University of Tokyo. The YAYOI reactor succeeded in virginal first criticality on April 10*th*, 1971, and it was the first fast-neutron reactor for research at a university in Japan. Various characteristic researches have been conducted by using fast neutrons generated through fission reaction without deceleration. After March 2011, it was decided to permanently stop the YAYOI reactor and decommissioning had been implemented. Using JENDL-4.0 evaluated data [5] and nominal neutron flux spectrum of the YAYOI reactor, Figure 2 shows the distribution of reaction rate per unit lethargy of ^{99}Tc. The peak of the reaction-rate distribution appears around 100 keV of neutron energy, which indicates that the distribution has sensitivity to regions where there are discrepancies between the libraries. Consequently, the authors thought that it would be possible to verify which evaluated nuclear data library was correct by examining integral experiment data of ^{99}Tc obtained by an activation method with the YAYOI reactor.

CONTACT Shoji Nakamura nakamura.shoji@jaea.go.jp Nuclear Data Center, Nuclear and LWR Engineering Division, Nuclear Science and Engineering Center, Japan Atomic Energy Agency, 2-4 Shirakata, Tokai-mura, Naka-gun, Ibaraki-ken 319-1195, Japan

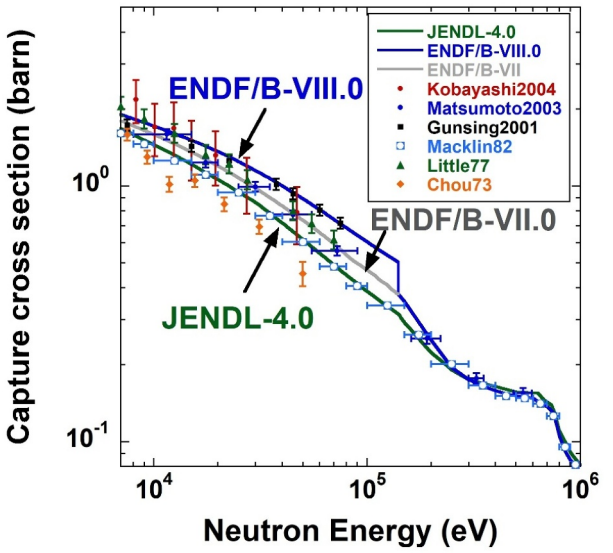

Figure 1. Situation of evaluated nuclear data libraries [5–7] and past experimental data [8–13] in the fast neutron energy region.

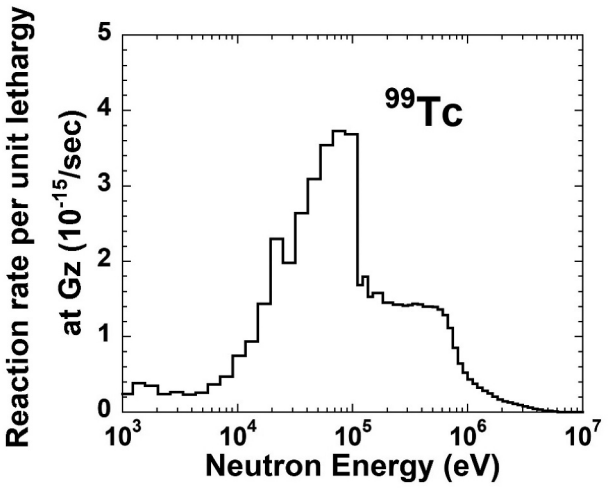

Figure 2. Distribution of reaction rate per unit lethargy of ^{99}Tc. The peak around 100 keV has a step in the shape because the lethargy width changes there.

2. Experiment

2.1. Method

The present experiment was performed by the activation method. A simplified decay scheme of the ^{99}Tc(n,γ)^{100}Tc reaction is drawn in Figure 3. First, an adequate amount (800 kBq) of ^{99}Tc sample is irradiated with reactor neutrons to generate ^{100}Tc. The produced ^{100}Tc decays with a half-life of 15.27 ± 0.05 sec [14] while emitting 540-keV and 591-keV decay gamma rays as shown in Figure 4, and then becomes stable ^{100}Ru. Next, the decay gamma rays are measured using a high-purity germanium detector and quantitatively analyzed. The present analysis used the emission probabilities for decay gamma rays, which were derived by the β-γ coincidence measurement in Ref [14]: 6.6 ± 0.5% for 540-keV and 5.5 ± 0.3% for 591-keV gamma rays. Reaction rates of ^{99}Tc are then obtained from yields of decay gamma rays. Finally, a neutron flux at an irradiation position is normalized with measured reaction rates of gold foils. The experimental reaction rate of ^{99}Tc is compared with calculated reaction rates using the evaluated nuclear data and the normalized neutron flux.

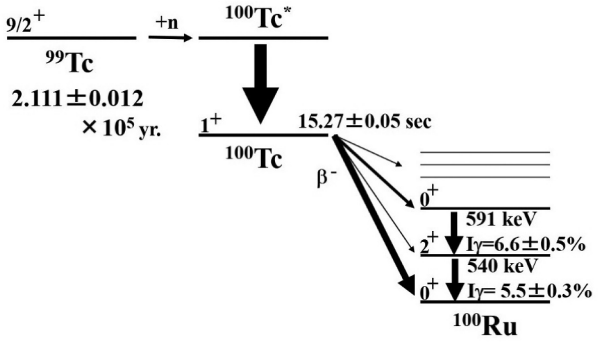

Figure 3. A simplified decay scheme of the ^{99}Tc(n,γ)^{100}Tc reaction.

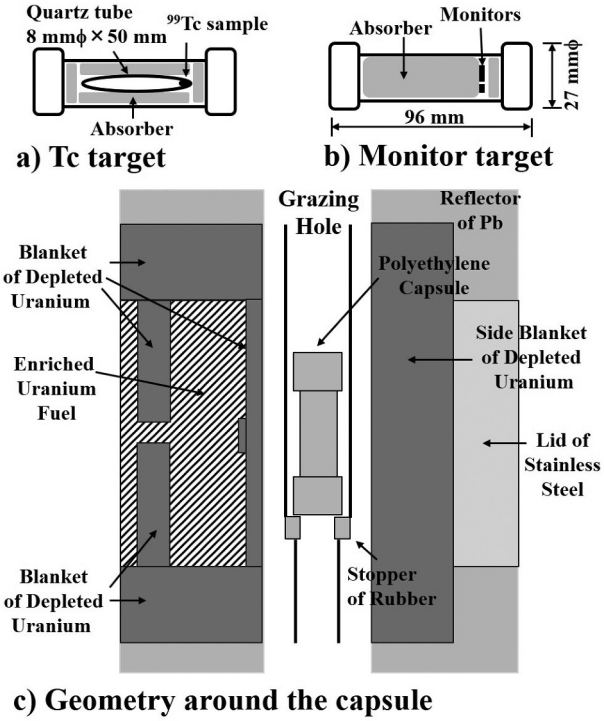

Figure 4. Outline of irradiation targets for the pneumatic system at the YAYOI reactor. (a) Tc target: the ^{99}Tc sample was encapsuled with the quartz tube. (b) Monitor target: neutron monitors are set at the same position as that in the ^{99}Tc sample. (c) Geometry around the capsule: the geometry was used for calculation of neutron spectrum at the irradiation position.

2.2. Target preparation

The standard solution of ^{99}Tc (TC99ELSA50; CERCA/LEA-AREVA, France) was used as samples for the

experiment. Its specific activity was 8.21 MBq/g sol. with uncertainty of 2% (1σ). Before the specific activity did not change after opening the ^{99}Tc solution-filled ampoule, a ^{99}Tc standard solution equivalent to 800 kBq in radioactivity was quickly extracted, and then gently dropped into the bottom of a high-purity quartz tube (8 mm in outer diameter, 50 mm in length). Immediately after that, the weight of the solution was measured by an electric balance, and the amount of ^{99}Tc was obtained from the weight and the specific activity. Such three ^{99}Tc samples were prepared. Information on the ^{99}Tc samples is summarized in Table 1. After the ^{99}Tc samples were sufficiently dried with an infrared lamp, the open end of each quartz tube was melt-sealed to form an ampoule. The ^{99}Tc ampoule was placed into a polyethylene capsule with a cushioning material. By packing the cushioning material in the capsule, the sample position was prevented from changing due to the impact during transfer for irradiation. This capsule is referred to as 'Tc target' hereinafter. An outline of irradiation targets is drawn in Figure 4. A piece of gold foil was placed as a neutron flux monitor in another polyethylene capsule at the same position as the ^{99}Tc sample to normalize a neutron flux for each day of irradiation. Furthermore, a set of neutron flux monitors was prepared such as scandium (Sc), copper (Cu) and manganese (Mn) suitable for examining capture reactions, and aluminum (Al), iron (Fe) and indium (In) for threshold reactions. The sets of them were put into other capsules to confirm the suitability of neutron flux spectrum at an irradiation position of the YAYOI reactor. The capsule containing the flux monitors is referred to as 'Monitor target.' Table 2 lists nuclear data used to analyze the monitors.

2.3. Neutron irradiation

The YAYOI reactor was used as a neutron source for neutron irradiation in the period: December 9th – 11th, 2008. The type of the reactor was a high enriched metal uranium fueled fast reactor cooled with air. The reactor power was rated at 2 kW and its fast-neutron flux was 10^{11} n/cm^2/sec. Figure 5 presents the cross-sectional view of the core structure of the YAYOI reactor. The reactor core was a high enriched metal uranium in a cylindrical disk, and its outside was surrounded with a depleted uranium blanket. Furthermore, this fuel part was housed in lead reflectors. The YAYOI reactor had a core assembly with a size of 0.5 m × 0.5 m × 7.3 m, and had two irradiation holes: one was the Glory hole (Gy) penetrating the core, and the other was the grazing hole (Gz) on the reflector side. An aluminum foil-holder was prepared for each irradiation hole, and the folder attached samples was loaded into the hole for neutron irradiation. The neutron flux at the Gy hole was larger and harder than that at the Gz hole because the Gy hole was located in the reactor core. It means that the Gy hole was more advantageous for irradiation with fast neutrons. In the present experiment, however, product ^{100}Tc has the short half-life of 15.27 ± 0.05 sec [14], and therefore it was necessary to measure gamma rays rapidly after irradiation. Since the Gz hole had

Table 1. Information on prepared ^{99}Tc samples and nuclear data [4].

Sample No.	Volume of solution (mg)	Radioactivity (kBq)	^{100}Tc half-life (sec)		γ-ray Energy E_γ (keV)	Emission Probability $I\gamma$ (%) [9]
1	102.7 ± 0.1	843.2 ± 16.9	15.8 ± 0.1	[4]		
2	106.1 ± 0.1	871.1 ± 17.4	15.27 ± 0.05	[14]*	539.59	6.5 ± 0.5
3	106.1 ± 0.1	871.1 ± 17.4	15.5 ± 0.1	[15]	590.83	5.5 ± 0.3

* This half-life data was used for the present analysis.

Table 2. Nuclear data of flux monitors used in the present work [4].

Nuclide	Shape and size	Weight * (mg)	Abundance and Purity (%)	Reaction	Half-life *	γ-ray Energy E_γ (keV)	Emission Probability I_γ* (%)
^{197}Au	Foil	9.6209 *1*	100	^{197}Au(n,γ)^{198}Au	2.6943 *3*	411.80	95.62 *6*
	0.01 mm^t	10.0472 *1*	99.9		(days)		
		9.2640 *1*					
^{45}Sc	Foil	15.1244 *1*	100	^{45}Sc(n,γ)^{46}Sc	83.79 *4*	889.28	99.984 *1*
	0.12 mm^t		99.9		(days)	1120.55	99.987 *1*
^{63}Cu	Wire	87.2223 *1*	69.17	^{63}Cu(n,γ)^{64}Cu	12.700 *2*	1345.84	0.473 *10*
	0.667 mm		99.9975		(hours)		
^{55}Mn	Foil	6.6313 *1*	100	^{55}Mn(n,γ)^{56}Mn	2.57878 *46*	846.77	98.87 *30*
	0.015 mmt		98.7		(hours)		
^{27}Al	Foil	12.7343 *1*	100	^{27}Al(n,p)^{27}Mg	9.458 *12*	843.76	71.8 *4*
	0.127 mm^t		99.992		(minutes)	1014.44	28.0 *4*
^{56}Fe	Foil	34.9393 *1*	91.68	^{56}Fe(n,p)^{56}Mn	2.57878 *46*	846.77	98.87 *30*
	0.127 mm^t		99.987		(hours)		
^{115}In	Foil	14.3283 *1*	95.7	^{115}In(n,n')^{115m}In	4.486 *4*	336.24	45.9 *23*
	0.125 mm^t		99.999		(hours)		

* In our notation, 9.6209 *1* is 9.6209 ± 0.0001, 2.6943 *3* is 2.6943 ± 0.0003, 95.62 *6* is 95.62 ± 0.06, and *etc.*

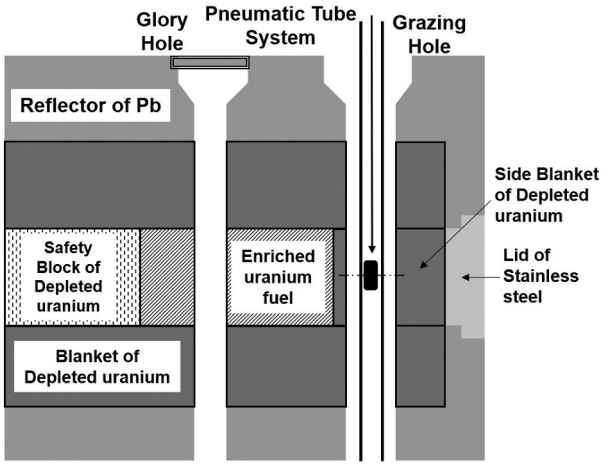

Figure 5. Cross-sectional view of the core structure of the Yayoi reactor. A type of the reactor is Uranium fueled, cooled fast reactor, and operated at 2-KW reactor power.

a margin of 56 mmϕ, it was possible to install a pneumatic system at the YAYOI reactor appropriately according to an experimental request. Consequently, we adopted the Gz hole for neutron irradiation because of the advantage of the pneumatic system.

During the present experiment, the YAYOI reactor was operated at 2-kW power. Neutron irradiations were performed in 3 sets during 3 days. Regarding the irradiation time, the irradiation time of 120 sec was changed to 60 sec after the 2nd set because the effect of dead time was large due to activation of impurities in the 1st set on the first day. The prepared three ^{99}Tc targets were sequentially irradiated, and then gamma-ray measurements were carried out. After waiting for ^{100}Tc to sufficiently decay out, irradiations and measurements were cyclically conducted. Before the shutdown of the daily reactor operation, the monitor target of the gold foil was irradiated for 5 min to check the fluctuation of the neutron flux. These processes were repeated as much as possible during the daily reactor operation in order to store statistics on gamma-ray yields, and finally repeated 74 times in 3 days. When the third set of Tc target was over, the monitor targets were irradiated to confirm the suitability of the neutron flux spectrum; a set of Al, Mn, and In monitors was irradiated for 3 min, and a set of Fe, Sc, and Cu monitors for 30 min. Discussions shall be given in *Subsection 3.1* on the suitability of the neutron flux spectrum by comparing calculated and measured values in reaction rates of the monitors. After the end of irradiations of ^{99}Tc samples, the soundness of the samples was confirmed to see if the samples had collapsed.

2.4. Gamma-ray measurement

The irradiated ^{99}Tc samples and the flux monitors were quickly collected at the injection site of the pneumatic system of the YAYOI reactor, and then gamma-ray measurement was performed for each ^{99}Tc sample. The flux monitors were measured on the same day after the measurements of all Tc samples. Decay gamma rays emitted from the irradiated Tc samples and flux monitors were measured with a high-purity germanium (Ge) detector (model GEM-90,240-P; ORTEC, United States) installed near the pneumatic system. A measurement distance was 150 mm from the front surface of the Ge detector to a sample. The gamma-ray peak efficiencies of the Ge detector were obtained with standard ^{152}Eu and ^{60}Co gamma-ray sources. The uncertainty of the ^{60}Co source was 1.5% (k= 2, extended uncertainty). The peak efficiency curve obtained with the ^{152}Eu source was calibrated with the ^{60}Co source. Decay gamma rays emitted from the irradiated ^{99}Tc samples were measured for 60 sec. Figure 6 draws an example of the gamma-ray spectrum obtained by the irradiated ^{99}Tc sample. Decay gamma rays originated to ^{100}Tc were observed at the gamma-ray energies of 540 keV and 591 keV. Although the statistical uncertainty of the gamma-ray yield was about 5~6% by only one measurement of the ^{99}Tc sample, statistical uncertainty was reduced by repeating irradiation and measurement 74 times.

3. Analysis and result

3.1 Neutron spectrum

For neutron irradiation with the pneumatic system, the YAYOI reactor provided polyethylene capsules with a size of 27 mmϕ×96 mm as shown in Figure 4. Concerned about thermalization of fast neutrons by the polyethylene capsule used for neutron irradiation, the staff of the YAYOI Management Department calculated a fast-neutron flux spectrum using a General Monte Carlo N-Particle Transport Code: MCNP [16] (*Version: 4 C, Library: FSXJ32A2*) with consideration of the polyethylene capsule and reactor geometry as

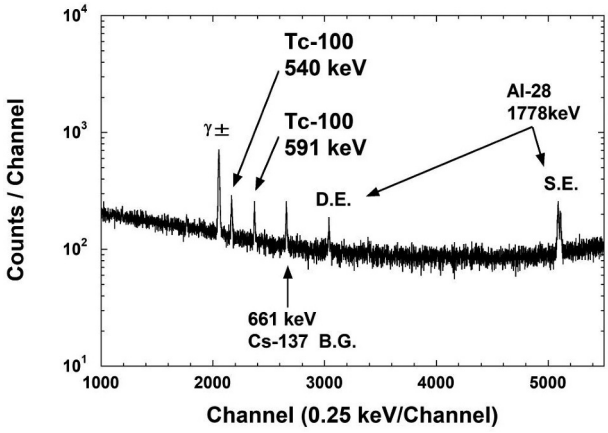

Figure 6. An example of gamma-ray spectrum of the irradiated ^{99}Tc sample.

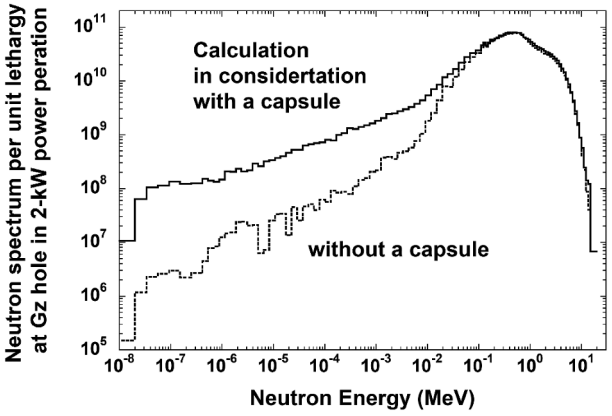

Figure 7. Farst-neutron flux spectrum thermalized by a rapid capsule in the Gz hole. Dashed line shows a nominal neutron spectrum in the Gz hole, solid line a neutron spectrum calculated in consideration with a rapid capsule.

drawn in Figures 4 and 5. The calculation results are plotted in Figure 7, where the dashed line shows a nominal fast-neutron flux spectrum in the Gz hole of the YAYOI reactor; the solid line a 'thermalized fast-neutron flux spectrum' obtained by considering the effect ascribe to the polyethylene capsule. For reference, the numerical data of the calculation results are listed in the Appendix. One finds that the calculated neutron flux component shows an increasing tendency in a low neutron-energy region due to thermalization of fast neutrons. This is because the polyethylene capsule itself actually acted as a moderator and thermalized fast-neutrons. The thermalization effect was very important. When using the nominal fast-neutron flux spectrum, a calculated reaction rate of a gold flux monitor is about 6 times underestimated with respect to an experimental one; conversely, the reaction rate should actually be 6 times larger. Using the thermalized fast-neutron flux spectrum, the calculated reaction rate for ^{99}Tc was enlarged by a factor of 2. These facts might demonstrate that fast neutrons can be thermalized effectively to improve transmutation rates by wrapping target nuclides with a moderator (polyethylene in this case) as described in Ref [2].

Before using the thermalized fast-neutron flux spectrum, its suitability should be further confirmed; it was made as follows. Experimental reaction rates R_E were obtained for the gold foil and flux monitors: Sc, Cu and Mn for the neutron capture reaction, and Al, Fe and In for the threshold reaction. The values R_E were then compared with calculated reaction rates R_C given with the calculated neutron flux spectrum and evaluated neutron cross-section data. The experimental value R_E was obtained by

$$R_E = \frac{\lambda \cdot Y}{\varepsilon_\gamma I_\gamma n_0 (1-\exp(-\lambda t_{irr})) \cdot \exp(-\lambda t_c) \cdot (1-\exp(-\lambda t_R))} \cdot \frac{t_R}{t_L}, \quad (1)$$

where the symbol n_0 is the number of nuclei in the target; I_γ is the gamma-ray emission probability; ε_γ is its gamma-ray detection efficiency; λ is the decay constant given by half-life $T_{1/2}$. In terms of time parameters, t_{irr} represents the irradiation time at the reactor, t_c the cooling time (or interval time) from the end of the irradiation to the start of measurement, t_R is a real time of gamma-ray measurement and t_L a live time; Y is the yield of gamma rays obtained by measurement. The calculated reaction rate R_C was obtained with the thermalized fast-neutron flux spectrum and evaluated neutron cross-section data, and written as follows:

$$R_c = \sum_{i=1}^{107} \sigma_i \phi_i \Delta u_i, \quad (2)$$

where the symbol σ_i is the reduced cross-section of 107 groups; ϕ_i is the 107-group neutron spectrum; Δu_i is the lethargy width. The evaluated libraries JENDL-4.0 [5] and JENDL/D-99 [17] were used for the cross-section data. These evaluated cross-section data were reduced to the 107 groups using a nuclear data processing code: NJOY [18]. The ratio (C/E) between calculated and experimental reaction rates is given by

$$C/E = G \cdot R_C/R_E, \quad (3)$$

where G is the self-shielding factor for neutrons, and written as

$$G = \frac{\sum_i \frac{1-\exp(-\rho\sigma_i d)}{\rho\sigma_i d} \sigma_i \phi_i \Delta u_i}{\sum_i \sigma_i \phi_i \Delta u_i}, \quad (4)$$

where ρ is the number of density of the sample, d is the sample thickness, and other symbols are the same as those in Eq. (2). Table 3 summarizes the calculated and experimental reaction rates for the neutron flux monitors. An average value of 0.985 was obtained from the results of the C/E in Table 3, and then the standard deviation of the average was estimated to be 0.020. The C/E ratio should be unity by nature; therefore, the difference of 0.015 between unity and the average value was also taken into account for uncertainty. The uncertainty was evaluated by the square root of the sum of squares using the deviation of 0.020 and the difference of 0.015, and then the C/E ratio was evaluated as 0.985 ± 0.025. Thus, the uncertainty of the calculated neutron flux spectrum was estimated to be 2.6%, and it was considered as one of the uncertainty factors affecting the integral experiments. Within this uncertainty, the thermalized fast-neutron flux spectrum with consideration of the effect by the polyethylene capsule was concluded to be appropriate and used for the present analysis.

3.2 Reaction rates of ^{99}Tc

After irradiation, decay gamma rays emitted from produced ^{100}Tc were measured with the Ge detector, and then production amount of ^{100}Tc was obtained

Table 3. Ratios (*C/E*) of reaction rates for the neutron flux monitors.

Reaction	R_C (1/sec)	R_E (1/sec)	Self-shielding factor*: G	Ratio *C/E*
^{197}Au(n,γ)^{198}Au	5.780×10^{-13} [a]	$(5.300 \pm 0.153) \times 10^{-13}$	0.914	0.997 ± 0.029 [a]
	5.689×10^{-13} [b]		0.920	0.988 ± 0.029 [b]
^{45}Sc(n,γ)^{46}Sc	1.510×10^{-14} [a]	$(1.716 \pm 0.048) \times 10^{-14}$	0.998	0.878 ± 0.025 [a]
	1.515×10^{-14} [b]		0.998	0.881 ± 0.025 [b]
^{63}Cu(n,γ)^{64}Cu	1.324×10^{-14} [a]	$(1.164 \pm 0.042) \times 10^{-14}$	0.995	1.132 ± 0.041 [a]
	1.277×10^{-14} [b]		0.997	1.094 ± 0.039 [b]
^{55}Mn(n,γ)^{56}Mn	1.540×10^{-14} [a]	$(1.525 \pm 0.044) \times 10^{-14}$	1.00	1.010 ± 0.029 [a]
	1.532×10^{-14} [b]		1.00	1.005 ± 0.029 [b]
^{27}Al(n, p)^{27}Mg	2.746×10^{-16} [a]	$(2.969 \pm 0.086) \times 10^{-16}$	1.00	0.925 ± 0.027 [a]
	2.808×10^{-16} [b]		1.00	0.946 ± 0.027 [b]
^{56}Fe(n, p)^{56}Mn	7.041×10^{-17} [a]	$(7.030 \pm 0.199) \times 10^{-17}$	1.00	1.002 ± 0.028 [a]
	7.044×10^{-17} [a]		1.00	1.002 ± 0.028 [b]
^{115}In(n, n')^{115m}In	- - -	$(1.526 \pm 0.089) \times 10^{-14}$	- - -	- - -
	1.440×10^{-14} [b]		1.00	0.944 ± 0.055 [b]

[a]JENDL-4.0 [5]
[b]JENDL/D-99 [17]
* Derived with Eq. (4).

from the yields of 540-keV and 591-keV gamma rays. The reported data for the half-life and gamma-ray emission probabilities [14] were used to calculate reaction rates of ^{99}Tc with Eq. (1). Figure 8 plots the results of the reaction rates obtained by the three sets of the irradiations and measurements, and also Figure 9 shows the reaction rates and their weighted averages for the three sets. The results of the reaction rates and their weighted averages are summarized in Table 4; their uncertainties were examined quantitatively as listed in Table 5.

3.3 Corrected C/E Ratio of ^{99}Tc

Here, the following definition shall be given to an 'average energy' for the reaction-rate distribution:

$$E_G = \frac{\sum_i \sigma_i \phi_i \Delta u_i E_{i,mid}}{\sum_i \sigma_i \phi_i \Delta u_i}, \tag{5}$$

where E_G is the average energy of the reaction-rate distribution; $Ei,_{mid}$ is the midpoint of the low energy E_i and upper energy E_{i+1} of the *i-th* energy group: the midpoint gives half the lethargy width. Consequently, the $E_{i,mid}$ is given by

$$E_{i,mid} = \sqrt{E_i \cdot E_{i+1}}. \tag{6}$$

Other symbols in Eq. (5) are the same as those in Eq. (2). The JENDL-4.0 library [5] was used to create the 107-group constants both for ^{99}Tc and for ^{197}Au. Table 6 lists the experimental and calculated reaction rates for ^{99}Tc and ^{197}Au and also the numerators in Eqs. (4) and (5). Using Eq. (5), the average energies E_G were derived as 85 keV for ^{99}Tc and 25 keV for ^{197}Au, respectively. Figure 10 plots the reaction-rate distributions for both ^{99}Tc and ^{197}Au. As seen from Figures 10, ^{197}Au has similar sensitivity to the neutron energy region of interest, therefore we considered normalizing the thermalized fast-neutron flux spectrum discussed in *Subsection 3.1.* with the C/E ratio of ^{197}Au. That is, the *C/E* ratio of reaction rates of ^{99}Tc between

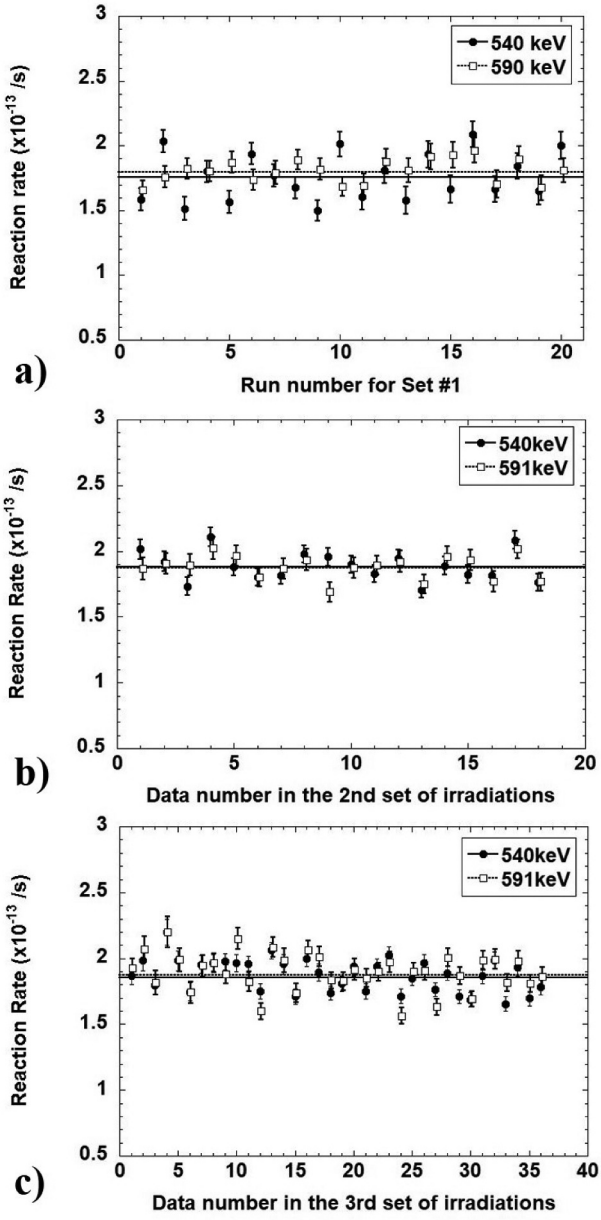

Figure 8. Experimental results of reaction rates for the three sets. The graphs show weighted averages of the data of reaction rates: (a) 20 data of reaction rates for the 1st set of experiments, (b) 18 data for the 2nd set, and (c) 36 data for the 3rd set. The symbol ● denotes the reaction rates obtained by the yields of gamma rays of 540 keV, and the symbol □ denotes those of 591 keV.

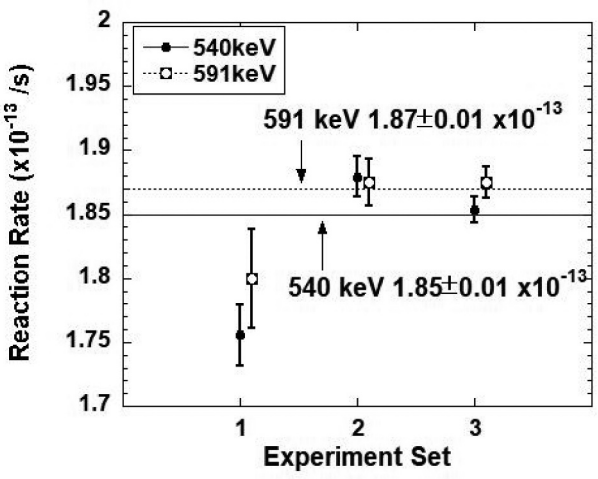

Figure 9. Weighted averages of reaction rates obtained from the yields of 540-keV and 591-keV gamma rays for three experimental sets. The uncertainties of the weighted averages in the figure are only statistical uncertainties.

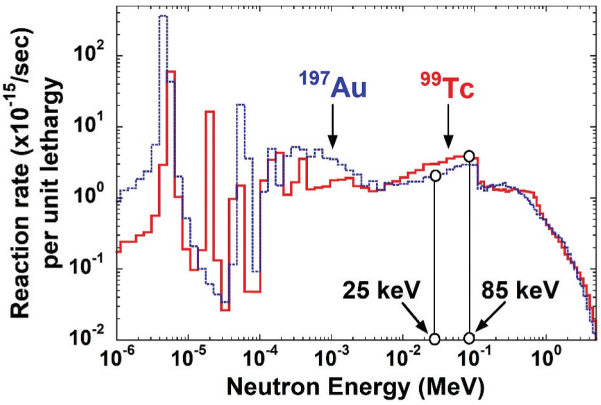

Figure 10. Average energies in reaction-rate distributions. Bold solid line shows the reaction rate distribution for Tc, dashed line for Au. Circles indicate what is called as 'average energy' of the reaction rate distribution.

Table 4. The results of reaction rates of ^{99}Tc and weighted averages.

	Reaction rate R_E (10^{-13} /sec)	
Experimental set	540 keV	591 keV
1^{st} set	1.756 ± 0.140	1.800 ± 0.119
2^{nd} set	1.880 ± 0.149	1.875 ± 0.118
3^{rd} set	1.853 ± 0.146	1.875 ± 0.118
Weighted average	1.849 ± 0.146	1.870 ± 0.117

the calculation and experiment was corrected by normalizing the neutron flux term as shown in the following equation:

$$(C/E)_{corr.} = \frac{(\mathrm{G}\cdot R_C/R_E)_{Tc}}{(\mathrm{G}\cdot R_C/R_E)_{Au}}. \qquad (7)$$

It is not necessary to include the uncertainty of the calibration source, and it is sufficient to just consider uncertainties due to fitting of the efficiency curve. That is, relative efficiencies are sufficient to consider the reaction rates for Eq. (7). The uncertainty due to the neutron flux spectrum would be canceled as well. Using the data in Table 6, the corrected C/E ratios were derived according to Eq. (7), and summarized in Table 7.

Table 5. Systematic uncertainties for ^{99}Tc sample and gold monitor measurements.

Considered Items	^{99}Tc sample	Uncertainties (%)	^{197}Au foil	Uncertainties (%)
Neutron flux spectrum		2.6		2.6
Half-life: $T_{1/2}$	15.27 ± 0.05 sec	0.59	$T_{1/2}$: 2.6943 ± 0.0003 days	0.01
Emission probability:	6.6 ± 0.5 for 540 keV	7.04	I_γ (%): 95.62 ± 0.06	0.06
I_γ (%)	5.5 ± 0.3 for 591 keV	5.17		
Weight: m (mg)	*ex.* 102.7 ± 0.1	0.1	m (mg): 9.621 ± 0.001	0.01
Specific activity (kBq)	*ex.* 843.2 ± 16.9	2.00	- - -	- - -
Peak Efficiency: ε_γ (%)	(fitting uncertainty only)	(0.71)	(fitting uncertainty only)	(0.86)
	fitting+source uncertainty	1.01	fitting+source uncertainty	1.14
Total systematic uncertainty:	for 540 keV	7.85 (7.38)		2.84 (0.86)
	for 591 keV	6.23 (5.62)		

*These systematic uncertainties due to the calibration source uncertainty and neutron flux spectrum are canceled at the time of division of reaction rates. The numbers in parentheses only consider the uncertainty due to the functional form of the efficiency curve.

Table 6. Reaction rates, self-shielding factors and average energies for ^{99}Tc and gold neutron monitor.

Reaction	R_E (10^{-13}/sec)	R_C (10^{-13}/sec)	Numerator in Eq. (4) (10^{-13}/sec)	Numerator in Eq. (5) (10^{-14} MeV/sec)	Self-shielding factor: G	Average energy E_G (keV)
^{99}Tc(n,γ)^{100}Tc	1.849 ± 0.140 [a] (±0.146)*	1.858[c] 2.018[d]	1.854	1.578	0.998	85
	1.870 ± 0.105 [b] (±0.117)*	1.994[e]				
^{197}Au(n,γ)^{198}Au	5.300 ± 0.046 (±0.153)*	5.780*	5.284	1.465	0.914	25

[a]540 keV
[b]591 keV * Numbers in parentheses denote total uncertainties.
[c]JENDL-4.0 library [5]
[d]ENDF/B-VII.0 [6], and
[e]‡ ENDF/B-VIII.0 [7]

4. Discussion

As seen from Table 6, the calculated reaction rate R_C obtained with JENDL-4.0 was almost in agreement with the experimental reaction rate R_E. The suitability of the neutron flux spectrum of the YAYOI reactor used for R_C was confirmed by examining the C/E ratios of the reaction rates for the neutron flux monitors in *Subsection 3.1*. In addition, the corrected C/E ratio in Table 7 was almost unity in the case of JENDL-4.0. The uncertainties due to the gamma-ray emission probabilities of ^{100}Tc is dominant; however, the principal values of the corrected C/E ratios are about 1σ apart each other. If the uncertainties in gamma-ray emission probabilities could be improved, the differences between the ratios would become more apparent. In terms of the results obtained by 591-keV gamma-ray with a slightly small uncertainty, the present simple integral experiments supported the JENDL-4.0 library.

Here, we consider whether or not ^{99}Tc sample preparation may fluctuate the principal values of the results in Tables 6 and 7. In the present sample preparation of ^{99}Tc, the specific activity of the standard solution had an accuracy of 2%, and even considering the likelihood of 2σ, the accuracy was 4%. The foregoing underestimation would be impossible; therefore, the suspicion of sample preparation would be denied. Furthermore, it can be considered that the loss of the sample due to repeated irradiation causes the reaction rate to decrease with each irradiation if there is a loss. The results in Figure 8 however did not show a downward trend in the reaction rates. Obviously, the soundness of the ^{99}Tc sample was confirmed after the irradiation. From the above reasons, it is considered that ENDF/B libraries might be overestimated beyond the uncertainty of the present result.

In this experiment, the pneumatic tube was used for the irradiations because of the short half-life of ^{100}Tc. The polyethylene capsule therefore thermalized the fast-neutron flux spectrum, which caused the reaction-rate distribution to broaden as shown in Figure 10. Conversely, if Tc targets are shielded with polyethylene or other moderator, the fast-neutron flux spectrum can be thermalized, and the reaction rate (or 'transmutation rate') would be increased by the contribution of reaction rates due to cross-sections in a resonance region. Thus, the calculated reaction rates *Rc* were examined with and without the polyethylene capsule, and the results are listed in Table 8 together with the experimental reaction rates R_E. One finds that the polyethylene capsule increased the reaction rate of ^{99}Tc by about 3 times, and also the experimental values R_E supported this. Consequently, we have experimentally demonstrated that the combined used of moderator with ^{99}Tc in the fast-neutron field in the YAYOI was advantageous for transmutation.

By using Glory hole where the neutron flux was harder than that in Grazing hole, the influence of thermalization may be suppressed and a sharp reaction-rate distribution may have been obtained. In this case, it may have been possible to discuss the cross-section using the same manner as Ref [19] within the width of the reaction-rate distribution. Instead, in this study, what is called as a 'spectral average cross section' was defined as follows:

$$\langle\sigma\rangle_C = \frac{\sum_i \sigma_i \phi_i \Delta u_i}{\sum_i \phi_i \cdot \Delta u_i} = \frac{R_C}{\sum_i \phi_i \Delta u_i}, \tag{8}$$

$$\langle\sigma\rangle_E = \frac{R_E}{\sum_i \phi_i \Delta u_i}. \tag{9}$$

The denominator $\Sigma\phi_i\Delta u_i$ in Eqs. (8) and (9) is an integrated neutron flux, and found to be 2.592×10^{11}(n/cm^2/sec) with capsule, and 2.585×10^{11}(n/cm^2/sec) without capsule, respectively. The results of spectral average cross-sections are also listed in Table 8. Since the difference in the integrated neutron flux was small, the spectral average cross-sections were three times larger than those in the case of no capsule. The spectral average cross-section is, of course, limited to a specific neutron flux, these results could be used to discuss the transmutation rate. Although the cross-sectional area is limited to a specific neutron flux, this result could be used to discuss the transmutation rate.

As shown in Figure 1, the JENDL-4.0 seems to adopt the data by Macklin *et al.* [10]. The ENDF/B-VII.0 adopted data reported by Little [9], Matsumoto [12] and Kobayashi *et al.* [13], and then the ENDF/B-VIII.0 adopted data by Gunsing *et al.* [11]. It is therefore undeniable that an unnatural

Table 7. Corrected C/E ratios of ^{99}Tc with evaluated libraries.

	(C/E) corr.	
Evaluated Nuclear Data Libraries	540 keV	591 keV
JENDL-4.0 [5]	1.006 ± 0.077	0.9947 ± 0.057
ENDF/B-VII.0 [6]	1.093 ± 0.083	1.081 ± 0.061
ENDF/B-VIII.0 [7]	1.080 ± 0.082	1.068 ± 0.061

Table 8. Reaction rates with/out capsule and spectral average cross-sections of ^{99}Tc.

	With capsule		Without capsule	
	$R_{E,C}$ (10^{-13}/sec)	$<\sigma>_{E,C}$ (mb)	R (10^{-13}/sec)	$<\sigma>_C$ (mb)
Present work	1.849 ± 0.140[a] 1.870 ± 0.105[b]	713 ± 54 [1)] 722 ± 41 [2)]	- - -	- - -
JENDL-4.0 [5]	1.858	717	0.6429	249
ENDF/B-VII.0 [6]	2.018	779	0.7010	271
ENDF/B-VIII.0 [7]	1.994	769	0.7723	299

$\Sigma\phi_i\times\Delta u_i = 2.592 \times 10^{11}$(n/cm^2/sec) with the capsule, 2.585×10^{11}(n/cm^2/sec) without the capsule.
[a]540 keV
[b]591 keV

Table 9. Outline of the past reported experiments.

Author	Method and Technique
Kobayashi et al. (2004) [13]	Neutron time-of -flight (TOF) method 46-MeV electron linear accelerator Bi_4GeO_{12} scintillators Energy range: 0.005 eV to 47 keV $^{10}B(n,\alpha\gamma)$ standard cross section Normalized with 22.9 ± 1.3(b) at 25.3 meV
Matsumoto et al. (2003) [12]	TOF method, Pulse-height weighting technique Pelletron accelerator A large anti-Compton NaI(Tl) spectrometer Energy range: 8 to 90 keV, 190, 330 and 540 keV ^{197}Au cross sections as a standard
Gunsing et al. (2001) [11]	TOF method, pulse-height weighing technique Pulsed white neutron source GELINA at Geel C_6D_6 detectors Energy range: 3 eV to 90 keV
Macklin et al. (1982) [10]	TOF method Oak Ridge Electron Linear Accelerator (ORELA) a pair of liquid scintillators Energy range: 2.65 to 2000 keV
Little and Block (1977) [9]	TOF method Linear accelerator at RPI 1.25 m-diam. Liquid scintillator, ^{10}B-NaI detector Energy range: 4 to 80 keV
Chou and Werle (1973) [8]	Slowing-down time spectrometer Energy range: 3 eV to 50 keV $^{10}B(n,\alpha)^7Li$, thermal cross section of ^{197}Au

estimation was performed around 150 keV in the evaluation of ENDF/B-VIII.0. Those experiments were performed with various detectors and techniques by the neutron time-of-flight method. The outline of the experiments is briefly summarized in Table 9. In order to measure relatively small cross-sections by the TOF method in a fast-neutron energy region, it is necessary to prepare a large amount of ^{99}Tc target. In the neutron energy region interested in this study, neutron scattering cross-sections of ^{99}Tc are much larger than capture cross-sections, and then it would be a question whether or not the contribution by neutron scattering was sufficiently considered in past TOF experiments. It is possible that the inadequate deduction of contributions by scattering neutrons caused an overestimation, which also caused the experimental data did not match each other in the range of neutron energy from a few keV to 100 keV. Consequently, it is desirable to re-measure or re-analyze the experimental data with the same experimental method and conditions in Table 9.

5. Conclusion

Using fast neutrons in the YAYOI reactor, we performed the integral experiments for the long-lived fission product ^{99}Tc by the activation method, and verified which library was correct among the three evaluated libraries: JENDL-4.0, ENDF/B-VII and VIII, which differed from each other in the keV neutron energy region. Technetium-99 samples and some neutron flux monitors were placed in the polyethylene capsules, and then irradiated with reactor neutrons in the Gz hole using the pneumatic system equipped with the YAYOI reactor. Irradiation of ^{99}Tc samples were repeated 74 times to accumulate statistics. The fast-neutron flux spectrum was calculated with the MCNP code with consideration of the thermalization effect by the polyethylene capsule. The appropriateness of the thermalized fast-neutron flux spectrum was checked by examining the C/E ratios of reaction rates for the monitors. The reaction rates of ^{99}Tc were obtained by measuring decay gamma rays emitted from ^{100}Tc. The thermalized fast-neutron flux spectrum was normalized with the experimental reaction rate of ^{197}Au and evaluated cross-section data. The experimental reaction rate of ^{99}Tc was compared with the reaction rates given using both the fast-neutron flux spectrum and evaluated nuclear data libraries. Although there have been discrepancies among three evaluated nuclear data libraries, the present integral experiments supported the evaluated nuclear data library JENDL-4.0.

In the process of the present experiments, the authors have experimentally demonstrated that the combined used of moderator with ^{99}Tc in the fast-neutron field was advantageous for transmutation.

Acknowledgments

The authors would like to greatly appreciate Professor Emeritus Yoshiaki OKA, Drs. Yuki ISHIWATARI (present affiliation: GE Hitachi), Isao SAITOH, Atsushi YASUMI, Tsutomu NAKAGAWA and Yukio MABUCHI of the University of Tokyo for their cooperation.

One of the authors (S.N.) would also like to express my gratitude to Dr. Osamu IWAMOTO of JAEA for the time and effort dedicated to his constructive and valuable comments.

This work has been carried out in part under a collaborative research project at Nuclear Professional School, School of Engineering, The University of Tokyo.

Disclosure statement

No potential conflict of interest was reported by the author(s).

ORCID

Yosuke Toh http://orcid.org/0000-0002-2494-5557
Hideo Harada http://orcid.org/0000-0002-9797-0745

References

[1] Chiba S, Wakabayashi T, Tachi Y, et al. Method to reduce long-lived fission products by nuclear transmutations with fast spectrum reactors. Sci Rep. 2017;7(1):13961.

[2] Wakabayashi T, Takahashi M, Chiba S, et al. Core concept of simultaneous transmutation of six LLFP nuclides using a fast reactor. Nucl Eng Des. 2019;352:110208.

[3] Wakabayashi T, Tachi Y, Takahashi M, et al. Study on method to achieve high transmutation of LLFP using fast reactor. Sci Rep. 2019;9(1):19156.

[4] Firestone RB, Shirley VS, Baglin CM, et al. Table of Isotopes. 8th ed. New York: John Wiley and Sons; 1995.
[5] Shibata K, Iwamoto O, Nakagawa T, et al. JENDL-4.0: a new library for nuclear science and engineering. J Nucl Sci Technol. 2011;48(1):1–30.
[6] Chadwick MB, Obložinský P, Herman M, et al. ENDF/B-VII.0 next generation evaluated nuclear data library for nuclear science and technology. Nucl Data Sheets. 2006;107(12):2931–3060.
[7] Brown DA, Chadwick MB, Capote R, et al. ENDF/B-VIII.0: the 8*th* major release of the nuclear reaction data library with CIELO-project cross sections, new standards and thermal scattering data. Nucl Data Sheets. 2018;148:1–142.
[8] Chou JC, Werle H. (n, γ)-Cross-section measurements of ^{99}Tc, Eu, Sm and Fe in the energy range 1 eV to 50 keV with a slowing-down time spectrometer. J Nucl Energy. 1973;27(11):811–823.
[9] Little RC, Block RC. Neutron capture cross-section measurements of ^{99}Tc up to 80 keV. Trans Am Nucl Soc. 1977;26:574.
[10] Macklin RL. Technetium-99 neutron capture cross section. Nucl Sci Eng. 1982;81(4):520–524.
[11] Gunsing F, Lepretre A, Mounier C, et al. Stellar neutron capture cross section of ^{99}Tc. Nuclear Physics A. 2001;688(1–2):496c–498c.
[12] Matsumoto T, Igashira M, Ohsaki T. Measurement of keV-neutron capture cross sections and capture gamma-ray spectra of ^{99}Tc. J Nucl Sci Technol. 2003;40(2):61–68.
[13] Kobayashi K, Lee S, Yamamoto S. Neutron capture cross-section measurement of ^{99}Tc by linac time-of-flight method and the resonance analysis. Nucl Sci Eng. 2004;146(2):209–220.
[14] Furutaka K, Nakamura S, Harada H, et al. Precise measurement of gamma-ray emission probabilities of ^{100}Ru. J Nucl Sci Technol. 2001;38(12):1035–1042.
[15] Harada H, Nakamura S, Katoh T, et al. Measurement of thermal neutron capture cross section and resonance integral of the reaction ^{99}Tc(n,γ)^{100}Tc. J Nucl Sci Technol. 1995;32(5):395–403.
[16] Briesmeister JF (*Ed.*) MCNP-A general monte carlo N-particle transport code version 4C, LA-12625-M; 2000.
[17] Kobayashi K, Iguchi T, Iwasaki S, et al. JENDL dosimetry file 99 (JENDL/D-99). Japan: Japan Atomic Energy Research Institute; 2002, JAERI 1344.
[18] MacFarlane RE, Muir DW. The NJOY data processing system, version 91. Los Alamos: Los Alamos National Laboratory; 1994. Technical Report No. LA-12740-M.
[19] Harada H, Nakamura S, Hatsukawa Y, et al. Measurements of neutron capture cross section of ^{237}Np for fast neutrons. J Nucl Sci Technol. 2009;46(5):460–468.

Appendix: Numerical information on fast-neutron spectra in the YAYOI reactor

Table A1. Fast-neutron spectral data with/without capsule in Figure 7.

Group No.	E_{Low} (MeV)	E_{High} (MeV)	Lethargy Width	Spectrum/Lethargy (1/cm^2/sec)	
				No Capsule	With Capsule
1	1.00000E-09	2.00000E-08	2.99573E+00	1.69552E+05	1.06352E+07
2	2.00000E-08	3.39750E-08	5.29893E-01	1.33720E+06	6.35026E+07
3	3.39750E-08	5.60160E-08	5.00012E-01	2.58799E+06	1.04482E+08
4	5.60160E-08	9.23570E-08	5.00024E-01	2.97252E+06	1.13445E+08
5	9.23570E-08	1.52280E-07	5.00059E-01	3.38814E+06	1.33901E+08
6	1.52280E-07	2.51080E-07	5.00051E-01	2.53112E+06	1.21928E+08
7	2.51080E-07	4.13990E-07	5.00070E-01	3.06026E+06	1.25968E+08
8	4.13990E-07	5.31580E-07	2.50012E-01	5.10612E+06	1.50580E+08
9	5.31580E-07	6.82560E-07	2.49997E-01	8.89203E+06	1.39141E+08
10	6.82560E-07	8.76430E-07	2.50006E-01	9.56241E+06	1.32935E+08
11	8.76430E-07	1.12530E-06	2.49948E-01	1.41030E+07	1.46538E+08
12	1.12530E-06	1.44500E-06	2.50060E-01	1.66884E+07	2.08594E+08
13	1.44500E-06	1.85540E-06	2.49991E-01	1.72839E+07	2.05274E+08
14	1.85540E-06	2.38240E-06	2.50008E-01	2.72188E+07	2.31155E+08
15	2.38240E-06	3.05900E-06	2.49980E-01	2.77511E+07	2.05354E+08
16	3.05900E-06	3.92790E-06	2.50017E-01	2.32956E+07	2.16958E+08
17	3.92790E-06	5.04350E-06	2.49995E-01	2.39287E+07	2.92752E+08
18	5.04350E-06	6.47600E-06	2.50003E-01	7.15907E+06	2.60380E+08
19	6.47600E-06	8.31530E-06	2.49994E-01	8.22158E+06	3.17158E+08
20	8.31530E-06	1.06770E-05	2.49995E-01	2.88095E+07	3.33285E+08
21	1.06770E-05	1.37100E-05	2.50034E-01	3.81180E+07	3.69198E+08
22	1.37100E-05	1.76040E-05	2.50001E-01	3.88834E+07	3.95928E+08
23	1.76040E-05	2.26030E-05	2.49957E-01	1.54764E+07	4.59771E+08
24	2.26030E-05	2.90230E-05	2.50006E-01	5.12509E+07	5.22843E+08
25	2.90230E-05	3.72660E-05	2.49993E-01	2.88903E+07	5.24037E+08
26	3.72660E-05	4.78510E-05	2.50011E-01	5.25723E+07	6.27734E+08
27	4.78510E-05	6.14420E-05	2.50002E-01	5.78590E+07	6.64546E+08
28	6.14420E-05	7.88930E-05	2.49999E-01	4.52054E+07	6.94370E+08
29	7.88930E-05	1.01300E-04	2.49994E-01	7.12152E+07	7.16404E+08
30	1.01300E-04	1.30070E-04	2.49986E-01	6.36652E+07	8.03815E+08
31	1.30070E-04	1.67020E-04	2.50041E-01	1.04506E+08	7.77058E+08
32	1.67020E-04	2.14450E-04	2.49963E-01	9.59693E+07	9.86068E+08
33	2.14450E-04	2.75360E-04	2.50003E-01	9.90127E+07	1.06824E+09
34	2.75360E-04	3.53570E-04	2.50002E-01	9.08077E+07	1.31647E+09
35	3.53570E-04	4.54000E-04	2.50016E-01	1.25545E+08	1.27026E+09
36	4.54000E-04	5.82950E-04	2.50004E-01	1.65085E+08	1.38683E+09
37	5.82950E-04	7.48520E-04	2.49996E-01	1.77971E+08	1.49063E+09
38	7.48520E-04	9.61120E-04	2.50001E-01	2.32368E+08	1.61993E+09
39	9.61120E-04	1.23410E-03	2.49998E-01	2.46801E+08	1.79469E+09
40	1.23410E-03	1.58460E-03	2.49990E-01	4.27583E+08	2.01773E+09
41	1.58460E-03	2.03470E-03	2.50016E-01	4.41356E+08	2.41003E+09
42	2.03470E-03	2.61260E-03	2.49998E-01	4.04305E+08	2.48239E+09
43	2.61260E-03	3.35460E-03	2.49987E-01	5.25667E+08	2.72174E+09
44	3.35460E-03	4.30740E-03	2.50002E-01	5.60674E+08	2.96656E+09
45	4.30740E-03	5.53080E-03	2.49998E-01	6.57440E+08	3.25684E+09
46	5.53080E-03	7.10170E-03	2.50002E-01	8.69960E+08	3.71628E+09
47	7.10170E-03	9.11880E-03	2.50004E-01	1.18825E+09	4.34028E+09
48	9.11880E-03	1.17090E-02	2.50020E-01	2.08123E+09	5.40850E+09
49	1.17090E-02	1.50340E-02	2.49957E-01	2.89031E+09	6.99403E+09
50	1.50340E-02	1.93050E-02	2.50050E-01	4.99932E+09	8.52244E+09
51	1.93050E-02	2.47880E-02	2.49996E-01	9.00315E+09	1.17108E+10
52	2.47880E-02	3.18280E-02	2.49987E-01	8.85925E+09	1.34345E+10
53	3.18280E-02	4.08680E-02	2.50001E-01	1.36611E+10	1.65116E+10
54	4.08680E-02	5.24750E-02	2.49990E-01	1.87898E+10	2.18634E+10
55	5.24750E-02	6.73790E-02	2.49996E-01	2.54302E+10	2.75352E+10
56	6.73790E-02	8.65170E-02	2.50008E-01	3.18612E+10	3.28547E+10
57	8.65170E-02	1.11090E-01	2.50000E-01	3.72362E+10	3.65640E+10
58	1.11090E-01	1.22770E-01	9.99720E-02	4.78332E+10	4.55817E+10
59	1.22770E-01	1.35690E-01	1.00060E-01	5.40936E+10	5.11064E+10
60	1.35690E-01	1.49960E-01	9.99957E-02	4.93939E+10	4.55032E+10
61	1.49960E-01	1.65730E-01	9.99914E-02	5.64410E+10	5.21407E+10
62	1.65730E-01	1.83160E-01	1.00000E-01	6.21244E+10	5.80268E+10
63	1.83160E-01	2.02420E-01	9.99846E-02	6.26480E+10	5.66234E+10
64	2.02420E-01	2.23710E-01	1.00006E-01	6.77977E+10	6.09632E+10
65	2.23710E-01	2.47240E-01	1.00009E-01	7.12678E+10	6.38904E+10
66	2.47240E-01	2.73240E-01	9.99910E-02	7.59665E+10	6.96173E+10
67	2.73240E-01	3.01970E-01	9.99772E-02	7.90014E+10	6.84387E+10
68	3.01970E-01	3.33730E-01	1.00005E-01	8.23571E+10	7.38737E+10
69	3.33730E-01	3.68830E-01	1.00004E-01	8.50428E+10	7.86139E+10
70	3.68830E-01	4.07620E-01	9.99996E-02	8.62694E+10	7.96476E+10

(*Continued*)

Table A1. (Continued).

Group No.	E_{Low} (MeV)	E_{High} (MeV)	Lethargy Width	Spectrum/Lethargy (1/cm^2/sec)	
				No Capsule	With Capsule
71	4.07620E-01	4.50490E-01	1.00000E-01	8.64573E+10	7.68969E+10
72	4.50490E-01	4.97870E-01	1.00003E-01	8.83111E+10	7.98878E+10
73	4.97870E-01	5.50230E-01	9.99974E-02	8.91566E+10	7.90374E+10
74	5.50230E-01	6.08100E-01	1.00003E-01	8.74267E+10	7.86522E+10
75	6.08100E-01	6.72060E-01	1.00008E-01	8.44741E+10	7.82760E+10
76	6.72060E-01	7.42740E-01	9.99984E-02	7.85116E+10	7.18284E+10
77	7.42740E-01	8.20850E-01	9.99944E-02	7.08878E+10	6.49681E+10
78	8.20850E-01	9.07180E-01	1.00000E-01	6.60360E+10	6.14239E+10
79	9.07180E-01	1.00260E+00	1.00011E-01	6.10104E+10	5.83526E+10
80	1.00260E+00	1.10800E+00	9.99600E-02	5.51524E+10	5.28915E+10
81	1.10800E+00	1.22460E+00	1.00058E-01	5.06628E+10	4.95770E+10
82	1.22460E+00	1.35340E+00	1.00006E-01	4.67319E+10	4.49932E+10
83	1.35340E+00	1.49570E+00	9.99744E-02	4.36280E+10	4.26652E+10
84	1.49570E+00	1.65300E+00	9.99975E-02	4.14143E+10	4.06526E+10
85	1.65300E+00	1.82680E+00	9.99740E-02	3.92709E+10	3.86526E+10
86	1.82680E+00	2.01900E+00	1.00037E-01	3.67514E+10	3.59329E+10
87	2.01900E+00	2.23130E+00	9.99821E-02	3.53218E+10	3.43766E+10
88	2.23130E+00	2.46600E+00	1.00013E-01	3.45203E+10	3.31037E+10
89	2.46600E+00	2.72530E+00	9.99811E-02	3.20152E+10	3.10702E+10
90	2.72530E+00	3.01190E+00	9.99926E-02	2.96993E+10	2.82967E+10
91	3.01190E+00	3.32870E+00	1.00011E-01	2.67872E+10	2.60167E+10
92	3.32870E+00	3.67880E+00	1.00005E-01	2.42695E+10	2.39872E+10
93	3.67880E+00	4.06570E+00	9.99993E-02	2.12450E+10	2.03312E+10
94	4.06570E+00	4.49330E+00	1.00001E-01	1.75109E+10	1.69144E+10
95	4.49330E+00	4.96590E+00	1.00007E-01	1.43086E+10	1.44824E+10
96	4.96590E+00	5.48810E+00	9.99876E-02	1.19268E+10	1.10917E+10
97	5.48810E+00	6.06530E+00	1.00002E-01	8.71810E+09	8.62580E+09
98	6.06530E+00	6.70320E+00	1.00001E-01	6.84053E+09	6.12027E+09
99	6.70320E+00	7.40820E+00	1.00002E-01	4.59643E+09	4.32678E+09
100	7.40820E+00	8.18730E+00	9.99967E-02	2.75628E+09	2.74790E+09
101	8.18730E+00	9.04840E+00	1.00004E-01	1.74104E+09	1.64499E+09
102	9.04840E+00	1.00000E+01	9.99972E-02	1.00468E+09	8.80067E+08
103	1.00000E+01	1.10520E+01	1.00026E-01	4.69258E+08	5.63612E+08
104	1.10520E+01	1.22140E+01	9.99714E-02	2.53205E+08	2.45423E+08
105	1.22140E+01	1.34990E+01	1.00033E-01	9.89192E+07	1.40810E+08
106	1.34990E+01	1.49180E+01	9.99530E-02	4.61975E+07	1.20373E+08
107	1.49180E+01	2.00000E+01	2.93164E-01	9.12954E+06	6.69380E+06